

N,N-Dialkylcarbamato complexes as precursors for the chemical implantation of metal cations on a silica support

Part 2.—Platinum(II) and its further reduction to platinum nanoparticles^{†‡}

Luigi Abis,^a Daniela Belli Dell' Amico,^b Carlo Busetto,^a Fausto Calderazzo,^{*b} Ruggero Caminiti,^c Carmine Ciofi,^d Fabio Garbassi^a and Guglielmo Masciarelli^{b,e}

^aEnichem S.p.A., Centro Ricerche Novara 'G. Donegani', Via G. Fauser 4, I-28100 Novara, Italy

^bUniversità di Pisa, Dipartimento di Chimica e Chimica Industriale, Sezione di Chimica Inorganica, Via Risorgimento 35, I-56126 Pisa, Italy

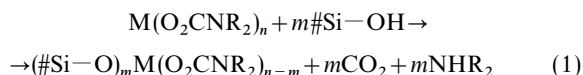
^cUniversità di Roma 'La Sapienza', Dipartimento di Chimica and Sezione Istituto Nazionale di Fisica della Materia (I. N. F. M.), P.le Aldo Moro 5, I-00185 Roma, Italy

^dUniversità di Pisa, Dipartimento di Elettronica, Informatica e Telecomunicazioni, Facoltà di Ingegneria, Via Diotisalvi 2, I-56126 Pisa, Italy

^eScuola Normale Superiore, Piazza dei Cavalieri 7, I-56100 Pisa, Italy

Implantation of platinum(II) on a commercial silica has been carried out under mild conditions by using *N,N*-dialkylcarbamato complexes as reactive precursors, in a biphasic liquid/solid system, carbon dioxide and secondary amine being released during the reaction with the acidic silanol groups of the support. Information about the coordination sphere of the silica-supported platinum(II) has been obtained by IR, XPS, solid-state NMR spectroscopy and WAXS measurements, which agree with chemical evidence. Reduction, either thermal or with dihydrogen, produces platinum nanoparticles, which were studied by conventional techniques and shown to be catalytically active in the hydrogenation of cyclohexene.

In the first paper of this series, some of us have shown^{1a} that *N,N*-dialkylcarbamato derivatives of tin(IV), of general formula $\text{Sn}(\text{O}_2\text{CNR}_2)_4$, are appropriate precursors for the implantation of this cation on silica.



This new method, represented by eqn. (1), is the chemical alternative to the better known ion implantation method^{1b} or to other chemical methods already reported in the literature:^{1c} it is based on the use of the generally soluble (in organic solvents) *N,N*-dialkylcarbamates for preparing metallosilicates, *i.e.* functionalized silicas containing surface-bonded transition metal cations. The advantages of using *N,N*-dialkylcarbamates (these compounds contain the metal–oxygen coordinative bond and are readily attacked by proton-active substances of even moderate acidity^{2a}) for this purpose are manifold: (a) availability of the starting compounds,^{2b–d} which can be prepared in any laboratory conventionally equipped for handling chemical substances under a controlled atmosphere; (b) the implantation reaction is prompt at room temperature and complete due to release of CO_2 ; (c) the other products of the reaction are easily transferred to the organic solvent used as medium. The chemical bonds thus formed through the interaction between the oxide support and $\text{M}(\text{O}_2\text{CNR}_2)_n$ allow a new surface coordination chemistry to be investigated. A limiting factor is the availability at a specific reactive site of a sufficient number of silanol groups [coefficient m of eqn. (1)] to perform the reaction with the metal precursor, whose oxidation number is given by coefficient n . For oxidation numbers >1 , the presence of residual carbamato groups around the surface-bonded cation is to be expected; this introduces the further

advantage of both spectroscopically monitoring the nature of the implanted species and, by exploiting the functionalities still present on the implanted cation, of carrying out further reactions.

We reckoned that the extension of this methodology to easily reduced metal cations such as platinum ($E^0 = 1.18 \text{ V}^3$) and palladium ($E^0 = 0.951 \text{ V}^3$) could introduce a further possibility, namely the reduction to the zerovalent state of the implanted cations and the consequent formation of metal particles.

This paper reports the implantation of platinum(II) on silica and its reduction, either thermal or chemical, to platinum nanoparticles. The data concerning palladium will appear in a forthcoming paper.⁴ Organometallics of transition and non-transition elements have been used extensively for the same purpose,⁵ but, to the best of our knowledge, this is the first time molecular compounds of platinum have been used for carrying out a highly chemoselective reaction with an oxide support, by operating in an organic solvent as medium under mild conditions.

Experimental

Materials and reagents

All solvents were purified and dried by conventional methods. All gaseous reagents were purchased as high purity gases. Unless otherwise specified, all operations were carried out under an inert gas or under pre-dried CO_2 , as required. Molecular sieves were dried at 200°C (*ca.* 10^{-2} mmHg) and then stored under an inert atmosphere.

All preparations and handlings involving the *N,N*-diethylcarbamato complexes were carried out under exclusion of moisture. Reagent grade silver oxide (Chimet SpA, silver content 93%), diethyl sulfide (Merck, $>98\%$), and aqueous solutions of $[\text{PtCl}_4]^{2-}$ (Chimet SpA) were used without further purification. Diethylamine (Janssen) was distilled from sodium

[†] Part 1: ref 1(a).

[‡] In partial fulfilment of the requirements for the PhD Thesis of G.M., Scuola Normale Superiore, Pisa.

under an inert atmosphere. The platinum(II) compound *cis*-PtCl₂(SEt₂)₂,⁶ was prepared as described in the literature, from an aqueous solution of [PtCl₄]²⁻ with diethyl sulfide in excess. PtI₂(Et₂NH)₂ was prepared by a slight modification of the literature procedure⁷ from PtI₂ and NHEt₂ in toluene suspension under dinitrogen; it was obtained⁸ as a mixture of the *cis* and *trans* isomers [¹H NMR ([²H₆]benzene, 22 °C, ppm from TMS): 3.5 s (br), 3.1 (m, 4 H), 1.9 (m, 4 H), 1.1 (t, 12 H); ¹⁹⁵Pt NMR ([²H₆]benzene, 23 °C, ppm from H₂PtCl₆ in water): -3970 and -3140]. The silver carbamate complex Ag(O₂CNEt₂) was prepared as described in the literature⁹ from Ag₂O and an excess of NHEt₂ in heptane with carbon dioxide at atmospheric pressure, in the presence of 4 Å molecular sieves as dehydrating agents; after filtration, the resulting solution (still containing the excess of diethylamine) was used for the subsequent reactions, after determination (Volhard) of the silver content.

Commercial silica (Grace, EP 17G, surface area, 325 m² g⁻¹; pore volume, 1.82 cm³ g⁻¹ or SD 3217/50, surface area, 318 m² g⁻¹; pore volume, 2.22 cm³ g⁻¹) was treated at 160 °C for 12 h or at 180 °C for 16 h *in vacuo* (10⁻² mmHg), giving, respectively, samples DB-14.214 and GM-222.2; treatment under reduced pressure eliminated most of the physisorbed and/or chemisorbed water; the silica samples thus obtained were then stored in flame-sealed vials under an atmosphere of dry CO₂.

The total silanol content [2.8 mmol g⁻¹ (sample DB-14.214) or 3.9 mmol g⁻¹ (GM-222.2)] was arbitrarily estimated from the mass loss by calcination at 850 °C. IR diffuse reflectance spectra of GM-222.2 show a sharp IR absorption at 3745 cm⁻¹ attributed to isolated silanol groups.¹⁰ After calcination at 850 °C, this absorption is even more evident, relative to the broad band in the 3000–3700 cm⁻¹ region. The silica treated at 160–180 °C for several hours has two intense ²⁹Si NMR peaks at -111 and at -102 ppm (relative to neat liquid SiMe₄), assigned to the Si(O-)₄ (Q4) and Si(OH)(O-)₃ (Q3) sites, respectively.¹¹ The resonance at -90 ppm attributed to geminal silanols Si(OH)₂(O-)₂ (Q2), is very weak.

Gas-volumetric and elemental analyses

The carbon dioxide content of the silica-supported platinum species and the carbon dioxide evolved in the course of the implantation reaction on silica were determined in a thermostatted gas burette, previously described,¹² using liquid media previously saturated with carbon dioxide at the temperature of the experiment.

C, H, and N analyses were carried out with a Carlo Erba model 1106 elemental analyzer at the Microanalytical Laboratory of the University of Pisa (Faculty of Pharmacy). Elemental analyses were carried out by inductively coupled plasma-mass spectrometry (ICP-AES) with a Perkin-Elmer Plasma II instrument (Pt), or by X-ray fluorescence (XRF) with a Philips PW 1404/10 instrument (S and Cl).

Instrumental analysis

IR spectra were measured with a FTIR Perkin-Elmer model 1725X instrument equipped with a KBr beam splitter and a TGS detector, in the range 4000–400 cm⁻¹, using CaF₂ windows for liquid samples and KBr or CaF₂ plates for Nujol mulls. Diffusion reflectance Fourier transform (DRIFT) spectra were measured with the same instrument by mixing the sample with dry KBr under an inert atmosphere and by rapid transfer to the cell (Spectra Tech). ¹H, ¹³C, and ¹⁹⁵Pt NMR spectra in solution were measured with a Varian Gemini 200 BB instrument.

Cross polarization magic angle spinning (CP MAS) ¹³C and ²⁹Si NMR spectra were measured at room temperature with a MSL 200 Bruker instrument operating at 50.321 and 39.760 MHz, respectively, chemical shifts being referred to TMS.

X-Ray photoelectron spectroscopy (XPS) spectra were measured with a Perkin-Elmer PHI 5500 ESCA system spectrometer equipped with a monochromatic X-ray source and an aluminium anode (Al-Kα radiation, 1483.6 eV), the source being maintained at 14 kV, with a 200 W power. The diameter of the sample area was *ca.* 400 μm and the background pressure in the analysis chamber was 10⁻⁸ Pa. Samples were mildly pressed on clean indium platelets and then introduced into the analysis chamber. Both operations were carried out under a dinitrogen atmosphere. For each sample, a preliminary general spectrum was recorded, in order to detect the presence of possible contaminants; the relevant photoemission peaks (Pt 4f, O 1s, C 1s, Si 2p) were then recorded under high resolution conditions. From the photoemission peak intensity, the surface atomic concentrations were estimated, using the elemental sensitivity factors method.¹³ Electrostatic charging was attenuated by using a low-energy flow electron gun; generally, peaks free from the typical deformations due to this phenomenon were obtained.

Transmission electron microscopy (TEM) images were obtained with a JEOL JEM 2010 instrument operating at 200 kV. A small amount of material was ground in a mortar until a very fine powder was obtained, which was deposited on a lacy carbon film supported on a standard copper grid. To avoid deterioration or contamination, the time required for sample preparation, carried out under a dinitrogen atmosphere, was reduced to a minimum (*ca.* 10 min). Bright field images were used in order to obtain the size distribution of platinum particles.

Wide angle X-ray spectroscopy (WAXS) and small angle X-ray spectroscopy (SAXS) data were collected with a non-commercial X-ray energy scanning diffractometer¹⁴ equipped with an X-ray generator (water-cooled tungsten target, 3.0 kW maximum power), a solid-state detector connected to a multichannel by means of an electronic chain, a collimator system, step motors and sample holder. The white Bremsstrahlung component of a standard Seifert X-ray tube was used at 45 kV and 35 mA. The energy interval was 13–38 keV; measurement angles (θ): 26, 21, 15.5, 10.5, 8, 5, 3.5, 3, 2, 1.5, 1, 0.5, 0.4, 0.3°; scattering parameter (q) interval, 0.07–16.9 Å⁻¹ (q = 0.05–0.2 Å⁻¹ for SAXS), with q = (4π/λ)sinθ, 2θ being the scattering angle, and λ the radiation wavelength. After the usual corrections of the experimental data,^{14b} the static structure function S(q) was obtained from the observed intensity I(E, θ). The Fourier transformation of the S(q) function gives the radial distribution function D(r):

$$D(r) = 4\pi r^2 \rho_0 + \frac{2r}{\pi} \int_{q_{\min}}^{q_{\max}} q S(q) M(q) \sin(qr) dq \quad (2)$$

In this equation, ρ₀ is the average electronic density of the sample {ρ₀ = [Σ_in_if_i(0)]²V⁻¹}, V is the stoichiometric unit volume, and M(q) is a sharpening factor defined as:

$$M(q) = \left\{ \frac{[\sum n_i f_i(0)]^2}{[\sum n_i f_i(q)]^2} \right\} \exp(-0.01 q^2) \quad (3)$$

The fitting of the experimental structure function was accomplished by using the Debye function *i*(q)¹⁵ and by adjusting the σ_{ij} and the r_{ij} parameters, where σ_{ij} is the r.m.s. variation of the interatomic distance r_{ij} {starting parameters: Pt–O, 2.045(7) Å; Pt–N, 2.075(7) and 2.085(6) Å [from *trans*-Pt(O₂CNEt₂)₂(NH₂)₂]^{8a}, Pt–S, *av.* 2.350(2) Å [from *cis*-Pt(SH)₂(PPh₃)₂]¹⁶ see also ref. 17 and 18}.

$$i(q) = \sum f_i(q) f_j(q) \frac{\sin(qr_{ij})}{qr_{ij}} \exp\left(-\frac{1}{2} \sigma_{ij}^2 q^2\right) \quad (4)$$

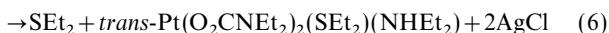
One of the thermally treated samples (GM-200/230), *vide infra*, was subjected to SAXS measurements, as the intensity of the scattered X-rays is related to the size of the scattering particles,

according to the Guinier law expressed by eqn. (5),¹⁹ where R_g is the gyration radius.

$$I(q) = I(0) \exp\left(-\frac{1}{3} R_g^2 q^2\right) \quad (5)$$

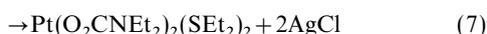
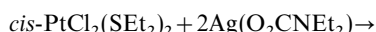
Chemical synthesis and implantation

Preparation of *trans*-Pt(O₂CNEt₂)₂(NH₂Et)₂(SEt₂) 1



Pre-dried molecular sieves (1.20 g) and Ag₂O (3.0 g, 12.95 mmol) were added to a solution of diethylamine (6.67 cm³, $d = 0.707 \text{ g cm}^{-3}$, 64.5 mmol) in toluene (210 cm³) maintained under carbon dioxide at atmospheric pressure and the resulting suspension was stirred at room temperature for 5 h. After filtration under carbon dioxide, an aliquot of the solution was titrated and the silver concentration was found to be $5.2 \cdot 10^{-2} \text{ M}$, corresponding to a 43% conversion of the starting silver oxide. Part of the solution, containing 9.35 mmol of silver and the excess of diethylamine, was treated with *cis*-PtCl₂(SEt₂)₂ (2.09 g, 4.68 mmol) under carbon dioxide. After 12 h stirring, AgCl (1.04 g, 78% of the expected amount) was filtered off and the filtrate was evaporated to dryness; the viscous oily residue was redissolved in pentane and the red microcrystalline solid precipitated by cooling to -18°C (Found: C, 36.7; H, 7.6; N, 7.1; S, 6.6. C₁₈H₄₁N₃O₄PtS requires C, 36.6; H, 7.0; N, 7.1; S, 5.4%; v/cm^{-1} (neat liquid) 3190(sh), 3056m, 2970–2872s, 1697 (probably due to some contamination by the corresponding carbonato complex), 1618s 1592s, 1576s, 1473s, 1461s, 1412s, 1375s, 1347w, 1302(sh), 1283s, 1229w, 1198s, 1156w; δ_{H} ([²H₈]toluene, 21 °C) 9.9 (1 H, s), 3.5 (8 H, q), 3.1 (4 H, m), 2.4 (4 H, m), 1.9 (6 H, t), 1.5 (6 H, t), 1.27 (12 H, t); δ_{C} ([²H₆]benzene, 21 °C) 47.9 [O₂CN(CH₂CH₃)₂], 41.9 [NH(CH₂CH₃)₂], 29.4 [S(CH₂CH₃)₂], 14.8 [O₂CN(CH₂CH₃)₂], 14.1 [NH(CH₂CH₃)₂], 12.4 [S(CH₂CH₃)₂]; δ_{Pt} ([²H₆]benzene, 21 °C, from H₂PtCl₆ in D₂O) –1953. Uncoordinated NH₂Et and SEt₂ exhibit the following NMR spectra: Et₂NH δ_{H} ([²H₆]benzene, 21 °C) 2.45 (4 H, q, CH₂), 0.97 (6 H, t, CH₃), 0.32 (1 H, s, NH); δ_{C} ([²H₆]benzene, 21 °C) 44.4 (CH₂), 15.6 (CH₃); SEt₂ δ_{H} ([²H₆]benzene, room temperature) 2.25 (4 H, t, CH₂), 1.07 (6 H, q, CH₃). Further ¹³C NMR data (O₂C) are listed in Table 1.

Preparation of Pt(O₂CNEt₂)₂(SEt₂)₂ 2



The platinum(II) complex *cis*-PtCl₂(SEt₂)₂ (3.95 g, 8.85 mmol) was dissolved in toluene (200 cm³) and solid Ag(O₂CNEt₂) (3.96 g, 17.7 mmol) was added under an atmosphere of dinitrogen. The contents of the reaction flask was maintained at 12 °C, protected from light and stirred magnetically. The reaction was monitored by both silver test and ¹⁹⁵Pt NMR spectra: after *ca.* 4 h the silver test in solution was negative

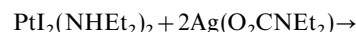
Table 1 ¹³C NMR data of the *N,N*-diethylcarbamato ligand O₂CNR₂ (R = Et) in complexes of platinum(II), palladium(II) and silver(I)

compound	δ (ppm) ^a	ref.
<i>trans</i> -Pt(O ₂ CNEt ₂) ₂ (NH ₂ Et) ₂ (SEt ₂) 1	164	this work
Pt(O ₂ CNEt ₂) ₂ (SEt ₂) ₂ 2	162	this work
<i>trans</i> -Pt(O ₂ CNEt ₂) ₂ (NH ₂ Et) ₂ 3	169	this work
<i>trans</i> -PtI(O ₂ CNEt ₂) ₂ (NH ₂ Et) ₂	166	8(a)
<i>trans</i> -Pd(O ₂ CNEt ₂) ₂ (NH ₂ Et) ₂	165	18
Ag(O ₂ CNEt ₂)	164	9

^aFrom TMS.

and only one ¹⁹⁵Pt resonance was detected in solution, while the starting platinum reagent was absent. The suspension was stirred for additional 5 h; the precipitate of AgCl was filtered off and the solution was evaporated to dryness under reduced pressure at room temperature yielding a viscous oil, which crystallized upon addition of pentane (100 cm³) and cooling to *ca.* -30°C (2.10 g, 39% yield). (Found: C, 32.1; H, 6.1; N, 3.6. C₁₈H₄₀N₂O₄PtS₂ requires C, 35.6; H, 6.6; N, 4.6%; v/cm^{-1} (PCTFE mull) 2973w, 2934w, 2876vw, 1697–1687w, 1611m, 1577(sh), 1472m, 1411m, 1376w; δ_{H} ([²H₈]toluene) 3.5 (8 H, m), 2.9 (4 H, m), 2.1 (4 H, m), 1.2 (12 H, t), 1.15 (12 H, t); δ_{C} ([²H₆]benzene, 20 °C) 42.0 [O₂CN(CH₂CH₃)₂], 30.8 [S(CH₂CH₃)₂], 14.8 [O₂CN(CH₂CH₃)₂], 12.4 [S(CH₂CH₃)₂]; δ_{Pt} ([²H₆]benzene, 20 °C, from H₂PtCl₆ in D₂O) –2982, with extensive decomposition during the acquisition time. Further ¹³C NMR data (O₂C) are listed in Table 1.

Preparation of *trans*-Pt(O₂CNEt₂)₂(NH₂Et)₂ 3



The platinum(II) complex PtI₂(NH₂Et)₂ (6.93 g, 11.64 mmol) was added to 225 cm³ of a 0.10 M toluene solution to Ag(O₂CNEt₂) (22.5 mmol) under a carbon dioxide atmosphere. After 5 d stirring, the suspension was filtered and the filtrate was evaporated to dryness and the resulting residue added to pentane (30 cm³). The orange product was collected by filtration and dried *in vacuo* (1.68 g, 26% yield). (Found: C, 37.7; H, 7.7; N, 9.7. C₁₈H₄₂N₄O₄Pt requires C, 37.7; H, 7.4; N, 9.8%; v/cm^{-1} (PCTFE mull) 3057m (br), 2977s, 2930m, 2878m, 1586m, 1563s, 1474s, 1458m, 1436w, 1411s, 1374ms, 1326mw, 1300s; δ_{H} ([²H₆]benzene, 20 °C) 9.7 (2 H, s), 3.2 (8 H, m), 2.8 (4 H, m), 2.0 (4 H, m), 1.7 (12 H, t), 1.0 (12 H, t). Single crystals (1,2-dimethoxyethane) were studied by X-ray diffraction at room temperature and gave the following space group and cell parameters²⁰ {data¹⁸ for [*trans*-Pd(O₂CNEt₂)₂(NH₂Et)₂] in braces}: $P2_1/c$ { $P2_1/c$ }, $a = 8.381(2)$ { $8.331(2)$ }, $b = 15.695(5)$ { $15.828(5)$ }, $c = 9.232(3)$ { $9.222(3)$ } Å; $\beta = 93.39(2)$ { $93.43(2)$ }°. The ¹³C NMR data (O₂C) are listed in Table 1.

Implantation

The reaction of compound 1 with silica is described in detail, the other reactions being carried out by a similar procedure. Table 2 reports yields and conditions of the implantation reaction. By operating under an argon atmosphere, silica (2.19 g, corresponding to 6.09 mmol OH and to a OH:Pt molar ratio of 5.9) was added at room temperature to a 0.052 M

Table 2 Implantation of platinum(II) on silica. Reaction conditions, yields and analytical data^a

precursor	molar ratio OH/Pt	label, Pt%	yield(%)
1	5.9	GM-67; 6.1 ^b	66
	18.2	GM-69; 2.9	99
2	8.3	GM-112; 4.3 ^c	66
	7.7	GM-200; 4.3 ^d	65
3	88.0	GM-238; 0.8	93

^aIn heptane for precursor 1 in toluene for precursors 2 and 3. Silica DB-14,214, except for GM-238 (silica GM-222.2). ^bN, 0.8; S, 0.9%; N/S, 2.0 (2.0); N/Pt, 1.8 (2.0); S/Pt, 0.9 (1.0); expected molar ratio in parentheses for the silica-bonded fragment #Pt(O₂CNEt₂)₂(NH₂Et)₂(SEt₂). ^cC, 4.2; N, 0.4; S, 1.6%; C/N 12.2 (13.0); C/S, 7.0 (6.5); N/S, 0.6 (0.5); N/Pt, 1.3 (1.0); S/Pt, 2.3 (2.0); expected molar ratio in parentheses for the silica-bonded fragment #Pt(O₂CNEt₂)₂(SEt₂)₂. ^dC, 4.1; N, 0.3; S, 1.5%; C/N, 15.9 (13.0); N/S, 0.5 (0.5); N/Pt, 1.0 (1.0); S/Pt, 2.1 (2.0); expected molar ratios in parentheses.

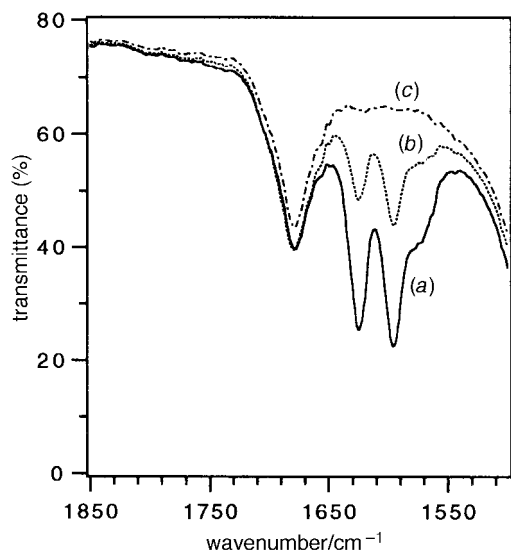
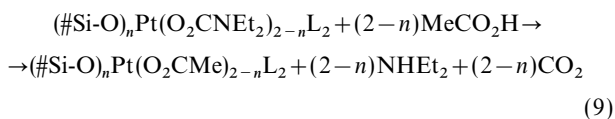


Fig. 1 Implantation of Pt on silica using *trans*-Pt(O₂-CNEt₂)₂(NHEt₂)(SEt₂), **1**, as precursor. IR spectra (0.1 mm CaF₂ windows, heptane): (a) before addition of silica; (b) after the first addition of silica (GM-67); (c) after the second addition of silica (GM-69).

solution of **1** in heptane (20 cm³). The colour of the initially red solution became immediately less intense and the resulting suspension was stirred for 4 h. The reaction was monitored by IR spectroscopy, which shows that the intensity of the bands around 1600 cm⁻¹, typical of the carbamato groups, had considerably decreased, Fig. 1(b). After filtration, the recovered yellow platinum-containing silica was washed with heptane (25 cm³), dried *in vacuo* at room temperature and kept in vials sealed under argon (sample GM-67). (Found: C, 6.7; H, 1.5; N, 0.8; Pt, 6.1; S, 0.9); ν/cm^{-1} (DRIFT) 2968m, 2938m, 2882w, 1602w, 1559w, 1504(sh), 1480m, 1461m, 1425m, 1381w, 1366vw, 1349vw, 1300w; the ¹³C CP MAS NMR spectrum is shown in Fig. 2.

The combined filtrate and washings from the preparation of sample GM-67 (total volume, 45 cm³), estimated to contain 0.36 mmol of platinum, was utilized for a further treatment with additional silica (2.36 g, 6.55 mmol of silanol groups, for a OH:Pt molar ratio of 18.2). The IR spectrum of the resulting supernatant solution, after 4 h stirring, showed the carbamato bands at about 1600 cm⁻¹ to be substantially absent, Fig. 1(c); the Pt/SiO₂ thus obtained is sample GM-69 of Table 2.

Sample GM-112 was subjected to chemical decomposition with acetic acid ($\text{p}K_{\text{a}}=4.76$ ²¹), eqn. (9), and the evolved carbon dioxide² was measured; material balance was in satisfactory agreement with expectations based on the quantitative data collected in the first step of the reaction (0.93 mol of CO₂ per mol of platinum were evolved).



Reduction processes

The reduction of silica-bonded platinum(II) was carried out both thermally and with H₂.

Thermal reduction. Several samples were subjected to thermal treatment *in vacuo* at 230 °C. For sample GM-112 the thermal evolution was followed at a range of temperatures from 60 to 230 °C. The volatile products (NHEt₂, Et₂S, H₂O) were collected in a cold (liquid nitrogen) trap and analyzed by ¹H NMR spectrometry; the solid platinum-containing residues

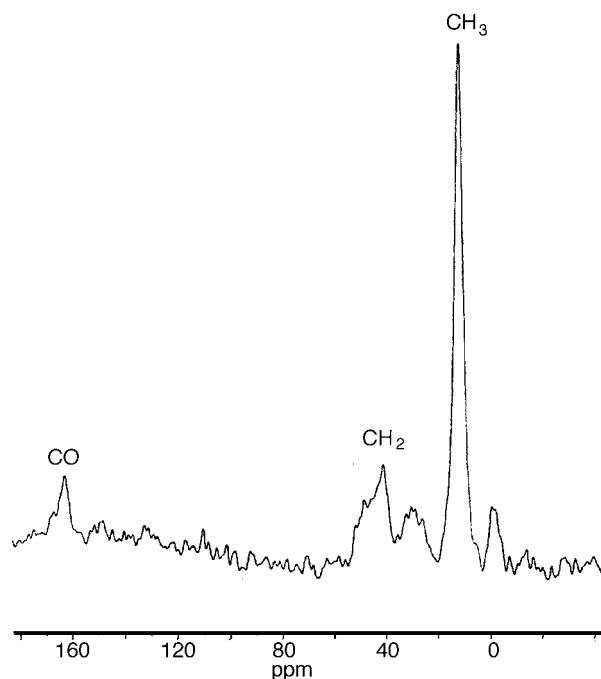


Fig. 2 ¹³C CP MAS NMR spectrum of Pt/SiO₂ (sample GM-67), see also Table 4. Irradiating field, 50 kHz; spinning rate, 5 kHz; contact time, 5 ms; sequence recycle time, 4 s; number of transients, 16640; spectral width, 20 kHz; time domain points, 512; chemical shifts are referred to TMS. Resonance at *ca.* 0 ppm is due to some contamination by silicone grease.

were collected and flame-sealed under argon, to be used for further studies (XPS, TEM, WAXS and SAXS measurements) and for the catalytic reactions. After thermal treatment, the samples retained some sulfur. Platinum and sulfur contents after the thermal treatment were determined by XRF for some of the samples of Table 3 (sulfur %, Pt/S molar ratio in parentheses): GM-112/230, 0.25 (2.8); GM-69/230, 0.1 (4.8); GM-200/230, 1.2 (0.6). No nitrogen or sulfur was detected by XPS for all thermally treated samples.

Reduction with dihydrogen. An aliquot of GM-112 was suspended in cyclohexane (25 cm³) and treated with dihydrogen at atmospheric pressure at 25.4 ± 0.1 °C. After 300 min stirring, the volume of absorbed dihydrogen had reached the asymptotic value corresponding to an H₂:Pt molar ratio of 1.0. In a separate experiment, another sample of GM-112 was suspended in [²H₆]benzene; after 48 h stirring under a dihydrogen atmosphere at room temperature, the supernatant liquid was examined by ¹H NMR spectroscopy: resonances due to

Table 3 Thermal reduction ^aof silica-bonded platinum(II)

sample/ temperature	XPS			TEM ^d d/Å
	E _b /eV	Pt atom% ^c	Pt/Si ^c	
GM-112/60	72.3	0.75	0.020	—
GM-112/100	72.3	0.75	0.021	12 ± 5
GM-112/140	72.3	0.78	0.021	11 ± 3
GM-112/180	72.5	0.67	0.018	15 ± 4
GM-112/230	71.2	0.44	0.012	26 ± 5
GM-200/230	71.0	0.40	0.010	—
GM-238/230	70.8	0.10	0.002	—
GM-69/190	—	—	—	30 ± 4
GM-69/230	71.6	0.40	0.011	—

^aUnder reduced pressure for 2 h, except for samples GM-200/230 (6 h) and GM-69/190 (3.5 h). ^bPt 4f_{7/2} binding energy (± 0.2 eV). Reference data (eV): Pt(s), 70.9; PtO, 73.8; Pt(OH)₂, 72.6.¹³ ^cIn all samples, the following E_b values (eV) were measured: O 1s, 533.1 ± 0.1; Si 2p_{3/2}, 103.7 ± 0.1. ^dPlatinum particle, mean diameter.

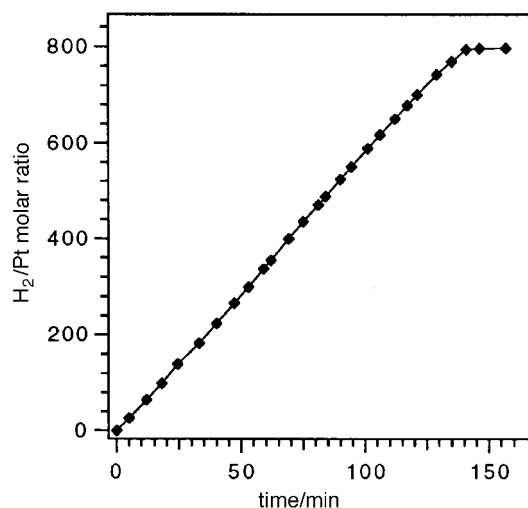


Fig. 3 Catalytic hydrogenation of cyclohexene for sample GM-238/230, see text. Solvent: cyclohexane; $T = 20.0 \pm 0.1$ °C; cyclohexene, 2.0 cm^3 (19.8 mmol). The plateau corresponds to a substantially quantitative conversion of the alkene.

both NHET_2 and SET_2 in an approximate molar ratio of unity were observed. In another experiment, a sample of GM-200 was heated at 100 °C under an atmosphere of dihydrogen: the volatile products were collected in a slow stream of dihydrogen, condensed in a cold trap (liquid nitrogen) and then dissolved in $[\text{D}_6]$ benzene; ^1H NMR peaks due to both NHET_2 and SET_2 were observed, with diethylamine being largely predominant. The sulfur content on the sample heated at 100 °C under H_2 was 0.8% (1.5% before heating, see Table 2), corresponding to a Pt/S molar ratio of 0.9 .

Catalysis

Several samples, after thermal treatment, showed catalytic activity in the hydrogenation of cyclohexene at room temperature and at atmospheric pressure. The catalytic hydrogenations were monitored by gas volumetry and mol of dihydrogen reacted as a function of time at constant temperature were determined. One of the hydrogenations is described in detail. A known amount of GM-238/230, containing 2.7×10^{-5} mol of platinum, was suspended in cyclohexane (15 cm^3); the pretreatment was carried out by stirring the system at 20.0 ± 0.1 °C under dihydrogen at atmospheric pressure after addition of cyclohexene (1 cm^3 , $d = 0.810 \text{ g cm}^{-3}$, 9.9 mmol). When the dihydrogen absorption was complete, 2.0 cm^3 of cyclohexene were added. Dihydrogen absorption was restarted, and was terminated after *ca.* 150 min, Fig. 3. The absorption of dihydrogen corresponded to a H_2/Pt molar ratio of *ca.* 800, with a substantially quantitative conversion of the alkene. A commercially available hydrogenation catalyst consisting of palladium supported on an aluminosilicate (Chimet D 9050, lot 81; 2 mass% Pd), previously activated by H_2 at room temperature, was used for comparison. Based on the volume of absorbed H_2 *vs.* time, our system was found to be about four times less active.

Results and Discussion

Precursors

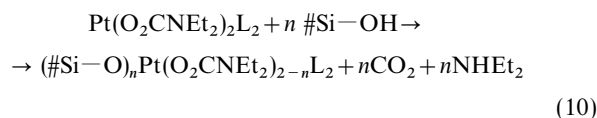
The syntheses of the platinum(II) precursors are represented in eqn. (6)–(8). By this methodology, compounds **1**–**3** have been prepared and utilized in the course of this work.

The choice of the platinum(II) reagent in reactions (6)–(8) was dictated by the requirement of reasonable rates in the $\text{X}^-/\text{O}_2\text{CNET}_2^-$ substitution as a consequence of the well known *trans* effect.²² Compound **3** has been established,

see Experimental section, to be isostructural^{8a} with the corresponding square-planar palladium(II) derivative,¹⁸ [*trans*- $\text{Pd}(\text{O}_2\text{CNET}_2)_2(\text{NHET}_2)_2$]. Thus, all platinum compounds utilized in this paper are believed to have a square-planar coordination, as expected for a cation of $5d^8$ electronic configuration; they all have a typical ^{13}C NMR spectrum with a resonance around 165 ppm, due to the carbon atom of the O_2CNET_2 group, Table 1. This resonance is not strongly affected by the nature of the supporting ligands and it has therefore been used as an important analytical tool to characterize the platinum-containing silica by ^{13}C CP MAS NMR spectra.

Implantation

The implantation process, Table 2, can be represented as follows ($n \approx 1$).



The reaction is fast at room temperature and the yield of the implantation reaction depends on the $\text{OH}/\text{Pt}^{\text{II}}$ molar ratio employed: with such a ratio as high as *ca.* 20, the implantation yield is substantially quantitative.

The analytical and spectroscopic data support a model of the platinum implantation on silica, whereby platinum(II) is associated with a silanolato group, while, statistically, one carbamate group is still retained in the coordination sphere of the cation, together with the neutral ligands originally present in the platinum(II) precursor. The oxidation state of II for platinum is confirmed by the XPS data (Table 4), while the presence of the carbamate ligand is confirmed by the ^{13}C NMR data (Table 4), and by the evolution of carbon dioxide in the presence of acetic acid, eqn. (9). About one mol of carbon dioxide per mol of platinum is evolved, thus showing that, statistically, the implantation reaction proceeds by one of the carbamate groups of the platinum(II) precursor interacting with the silanol sites.

WAXS data of sample GM-67, Fig. 4, can best be accommodated by a model with a platinum(II) centre in a square-planar coordination, the four coordination sites consisting of two oxygen atoms from the silanolato and the monodentate carbamate groups, the sulfur atom of SET_2 and the nitrogen atom of NHET_2 , Fig. 5. The Pt–O distance to the silanolato ligand of the support (2.15 \AA) is comparable to those found in several metal carbonyl fragments supported on γ -alumina [$\text{Ru}^{\text{II}}-\text{O}$ 2.17 \AA ,²³ $\text{Rh}^{\text{III}}-\text{O}$, 2.12 \AA ,²⁴ $\text{Rh}^{\text{III}}-\text{O}$, 2.04 \AA ,²⁵], on silica [$\text{Ru}-\text{O}$ 2.08 \AA ,²⁵] or on magnesia [$\text{Re}-\text{O}$ 2.15 \AA ,²⁶ $\text{Re}-\text{O}$ 2.13 \AA ,^{27a}].

The presence of coordinated ligands around platinum(II) is also in agreement with the detection of the organic ligands among the products intercepted at low temperature during the reduction of the silica-supported platinum(II) operated both thermally and with dihydrogen (*vide infra*).

Table 4 Spectroscopic data of silica-supported platinum(II)

precursor, label	XPS ^a E_b^a/eV	^{13}C NMR ^b [δ (ppm)]	^{29}Si NMR ^c [δ (ppm)]
1 , GM-67	72.4	162.9	–111; –102
GM-69	72.4	—	—
2 , GM-112	72.2	—	—
GM-200	72.7	163.3	—
3 , GM-238	72.8	—	—

^aSee Table 3, footnote b, for reference E_b values. ^b ^{13}C CP MAS NMR spectra, chemical shifts relative to TMS. ^c ^{29}Si CP MAS NMR spectra, chemical shifts relative to TMS, see text for assignment.

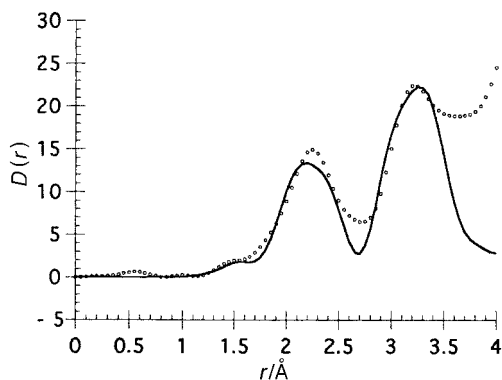


Fig. 4 WAXS data. Difference of the experimental radial functions of GM-67 and of the silica support. $D(r)$ values (—) were calculated by using the Debye formula and the interatomic parameters, as indicated in the text.

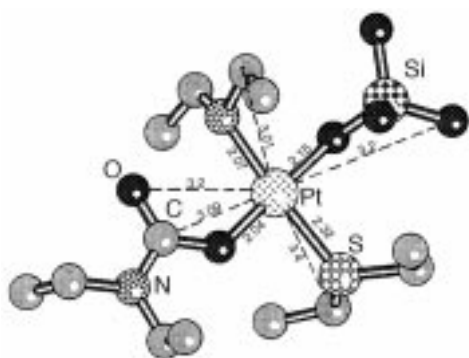


Fig. 5 Proposed model for the silica-bonded platinum(II) sample GM-67, originated from $trans\text{-Pt}(\text{O}_2\text{CNET}_2)_2(\text{SEt}_2)(\text{NHET}_2)$. **1**: the square-planar coordination consists of monodentate carbamate and silicate groups, diethylamine and diethylsulfide. Bond distances and interatomic non-bonding distances (Å) correspond to the best fit of the experimental WAXS data, see text for appropriate references.

Reduction

Thermal reduction. The thermally treated sample GM-112 generated volatile products identified as NHET_2 and SEt_2 . The XPS results on the solid residue thus obtained add some further insight into the thermal process. The absence of both nitrogen and sulfur at temperatures $\geq 60^\circ\text{C}$ suggests that the organic ligands are readily eliminated.

The reduction of platinum(II) to platinum(0) and the aggregation to platinum particles is evidenced by the XPS data [E_b 70.8–71.2 eV] of Table 3 showing that the samples treated at the highest temperature (230°C) exhibit a Pt $4f_{7/2}$ binding energy close to that of bulk metal (70.9 eV).¹³ It is interesting that for platinum on silica, a value of E_b of 71.3 eV has been reported by Che and coworkers,^{27b} and by Jackson *et al.*^{27c}

Fig. 6 shows some prominent XPS parameters as a function of temperature, namely Pt E_b , full width at half maximum (FWHM) relevant to Pt peaks, difference between silicon and Pt E_b values ($\Delta E_{\text{bSi-Pt}}$), and Pt/Si atomic ratios. The FWHM values of Fig. 6 are similar to those reported (6.3 eV) in a recent study of a Pt/SiO₂ system.^{27d} The ($\Delta E_{\text{bSi-Pt}}$) values confirm that real differences are observed, rather than artifacts due to charging of the samples. Thermal treatment causes significant changes at 180°C and above; in particular, reduction of platinum(II) to platinum(0) is indicated by the decrease of Pt E_b to a value close to that of platinum metal (70.9 eV),¹³ however, the increasing value of FWHM at higher temperature suggests that more species are present, for instance some residual platinum(II) or some metal particles interacting with the support.^{27e} It should be pointed out that XPS characterization of metal particles supported on an insulator is a challeng-

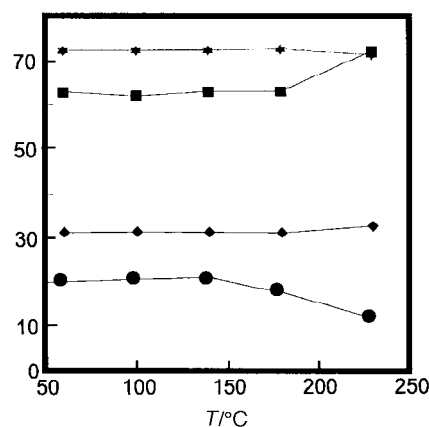


Fig. 6 XPS parameters for sample GM-112 as a function of temperature, see also Table 3 [from the top: binding energy (E_b) for platinum (*); in eV; full width at half maximum (FWHM) of Pt peak (■); in eV $\times 10$; $E_b(\text{Si}) - E_b(\text{Pt})$ (◆); in eV; Pt/Si (●; atom/atom $\times 1000$)].

ing issue.^{27d} The apparent decrease of the platinum content should correspond to particle growth. In fact, in evaluating parameters such as platinum surface concentration (Pt atom%, Table 3) or the Pt/Si atomic ratio, one must consider that XPS is a surface technique and the escape depth, which depends on the electron energy and on the nature of the sample, can be evaluated to be ca. 20–30 Å,^{27e} i.e. of the same order as the particle size (Table 3) in our case. Small particles contribute totally to the XPS peak intensity, while larger particles contain a non-contributing fraction of the metal, since it is located too deeply.

The loss of the platinum-coordinated ligands is further evidenced by the diffuse reflectance spectra showing a progressive decrease of the IR absorptions in the 1500–1300 cm^{-1} region upon heating *in vacuo* from 60 to 230°C , Fig. 7.

The secondary amine NHET_2 detected among the volatile products from the GM-112 sample [obtained from precursor **2**, i.e. from $\text{Pt}(\text{O}_2\text{CNET}_2)_2(\text{SEt}_2)_2$] must originate from the surface platinum-bonded carbamate group due to thermally promoted condensation of silanol groups to water, followed by hydrolysis of the platinum-bonded ligand (with release of free or platinum-bonded NHET_2). If this is the fate of the carbamate groups, by considering that thermal reduction was also observed for sample GM-238/230 (which originates from precursor **3**), the most reasonable explanation for the observed reduction of the silica-supported platinum(II) to platinum(0) involves the predominant participation in this process of

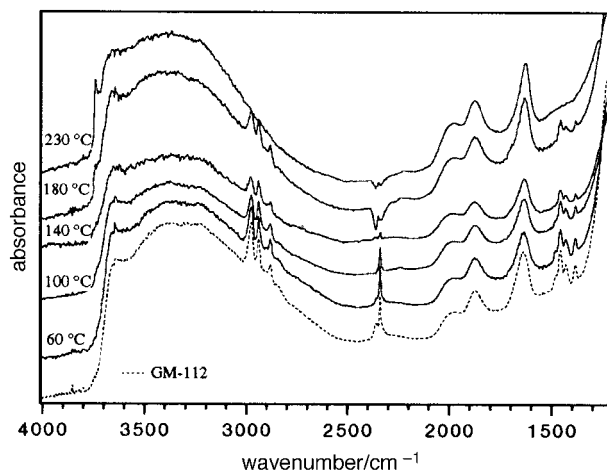
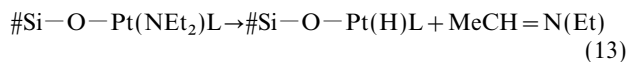
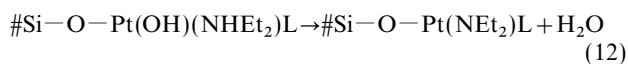
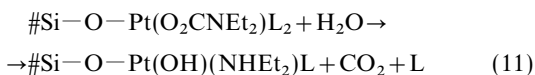


Fig. 7 DRIFT spectra of sample GM-112, subjected to *in vacuo* thermal treatments, in comparison with the untreated substance (bottom). The IR bands of the carbamate group around 1600 cm^{-1} are obscured by the absorptions due to the silica matrix.

platinum-bonded NHEt_2 . Presumably β -hydrogen elimination involving the ethyl group of the diethylamido group is responsible for the observed products. The formal two-electron transfer process from platinum-bonded hydride to oxygen-bonded proton would lead to platinum(0), eqn. (11)–(14).



β -Hydrogen elimination processes involving alkyl-transition metal bonds are well established in the literature,²⁸ whereas similar processes for dialkylamido,²⁹ alkoxo,³⁰ and thiolato³⁰ ligands have been relatively less studied.

Formation of reduced platinum is further substantiated both qualitatively (all samples darkened on heating) and quantitatively (DRIFT spectra on samples treated with CO, WAXS measurements). Chemisorption after exposure of the reduced sample to carbon monoxide at atmospheric pressure was observed spectroscopically: the DRIFT spectra of three samples are shown in Fig. 8; the carbonyl stretching vibration is close to that observed for CO linearly coordinated to a platinum surface ($2040\text{--}2080\text{ cm}^{-1}$).^{31a-f} Relevant to this point is the observation^{31g-j} that the carbonyl stretching vibration associated with the terminal carbonyl groups in the $[\text{Pt}_3(\mu\text{-CO})_3(\text{CO})_3]_n^{2-}$ anions increases as the nuclearity increases, the upper value of the series being 2065 cm^{-1} for $n=6$, which is close to the value observed for CO chemisorbed on platinum.^{31f,27b}

The reduction of platinum(II) was verified by WAXS measurements and the average particle size was also determined by SAXS. It is important to realize that TEM and WAXS (SAXS) measurements were carried out on two samples (GM-112/230 and GM-200/230, respectively), which were obtained from the same platinum(II) precursor and have the same platinum loading, thus allowing the results to be directly compared. The structure function obtained from the WAXS data of GM-200/230 is significantly different from that of the silica support, Fig. 9: this is a strong qualitative evidence that supported platinum nanoparticles strongly affect the scattering

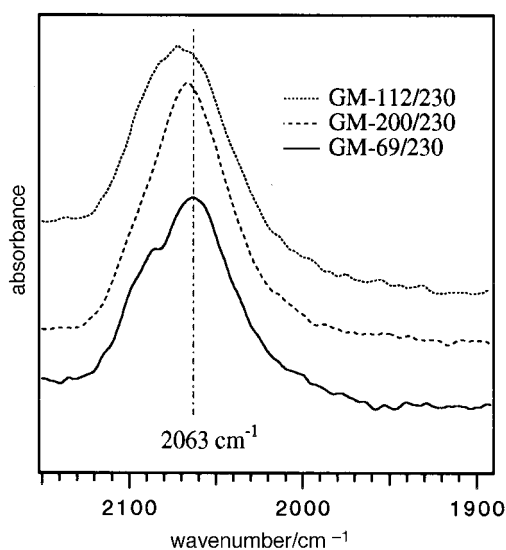


Fig. 8 DRIFT spectra of thermally reduced silica-supported platinum samples after exposure to carbon monoxide at atmospheric pressure and room temperature

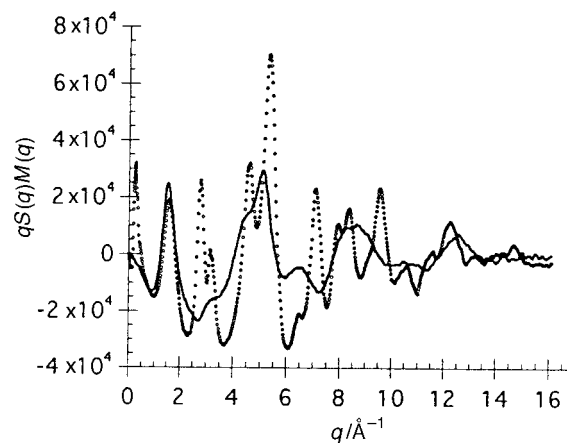


Fig. 9 WAXS data: observed $qS(q)M(q)$ values vs. q of silica support (—) and sample (···) GM-200/230

properties of silica, unlike the case of supported platinum(II). Although the structure function of silica is strongly affected by the presence of reduced platinum, it is reasonable to assume that the structural features of the silica framework are not significantly changed since the platinum particles are on the surface and their interaction with silica is limited to the platinum/silica interface. In this connection, it is interesting to note that, if the model of reduction proposed above, eqn. (11)–(14), is correct, the silica support is reconstituted from a chemical viewpoint [see formation of silanol sites according to eqn. (14)], although some water may be lost during the thermal reduction.

The difference of the experimental radial functions of sample GM-200/230 and the silica support is shown in Fig. 10. Several peaks appear in the radial plot, the main ones being observed at ca. 2.7, 3.9 and 4.9 Å, corresponding, respectively, to the platinum–platinum distances of the twelve nearest (2.775 Å), the six second-nearest (3.924 Å), and the twenty-four third-nearest (4.806 Å) neighbours of the fcc crystal lattice of bulk platinum³² ($a=3.9231\text{ Å}$), the twelve fourth-nearest neighbours being at 5.549 Å.

Evidence of the formation of nanometric particles by thermal treatment was obtained by TEM, Table 3. As expected, the particle size increases upon increasing the temperature. Fig. 11 shows a bright-field micrograph of a platinum/silica sample (GM-112/230) and Fig. 12 the relevant histogram of the size distribution obtained from the electron micrographs, with a log-normal distribution. It is generally accepted in small particle statistics that size is distributed log-normally,³³ according

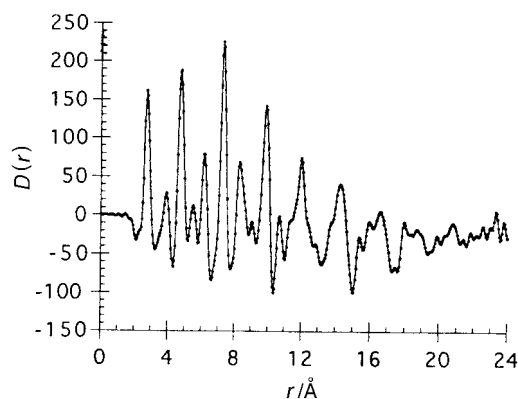


Fig. 10 WAXS data: difference of the experimental radial functions of GM-200/230 and of the silica support. Peaks at 2.7 Å, 3.9 Å and 4.9 Å are interpreted as platinum–platinum distances (see text).

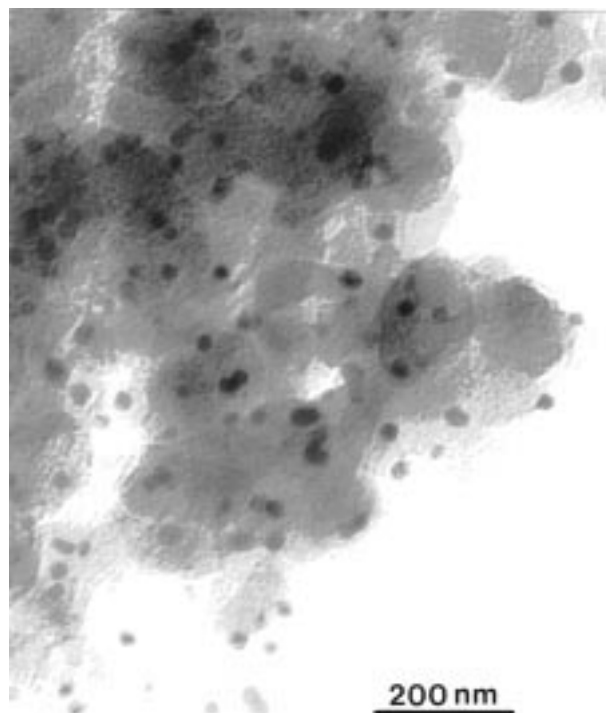


Fig. 11 Bright-field micrograph of GM-112/230, see also Table 3. Platinum particles appear as darker regions within the silica matrix.

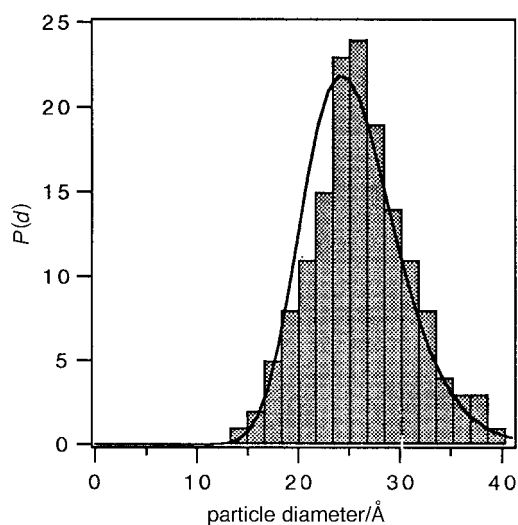


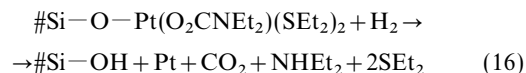
Fig. 12 Histogram of size distribution from TEM measurements of sample GM-112/230. The full line corresponds to the best fit of a log-normal distribution³³ ($d_0 = 24.3 \text{ \AA}$, $\sigma = 0.18$).

to eqn. (15), where d_0 is the geometric mean of the diameter and σ is the square root of the variance of the distribution.

$$P(d)/P(d_0) = \exp \left[-\frac{1}{2\sigma^2} \ln^2 \left(\frac{d}{d_0} \right) \right] \quad (15)$$

The mean diameter ($d_0 = 24.3 \text{ \AA}$), obtained by fitting the experimental size distribution, is only slightly smaller than that reported in Table 3 for the same sample. Similar size distributions in small metal particles have been reported in the literature.³⁴ The mean diameter for sample GM-112/230 ($26 \pm 5 \text{ \AA}$, Table 3) can be compared with that ($36 \pm 4 \text{ \AA}$) obtained from SAXS data for sample GM-200/230, which was prepared from the same precursor with the same loading (diameter determined by Guinier extrapolation¹⁹ with the assumption of spherical shape).

Reduction with dihydrogen. The reduction can be represented to a first approximation by the idealized stoichiometry of eqn. (16), the assumption being that the silanol groups are reconstituted during this process.



Of course, owing to the different adsorption properties of silica and reduced platinum with respect to NHEt_2 and SEt_2 , no relation can necessarily be found between the observed and the expected amounts of evolved organic products.

The absorption of dihydrogen corresponds to the theoretical amount expected for the formation of platinum(0) with no detectable extra absorption due to platinum-bonded hydride, thus suggesting that the aggregation to platinum particles is fast even at room temperature.

Catalysis

The presence of thermally reduced platinum is further evidenced by the catalytic activity in the hydrogenation of cyclohexene. Of course, the presence of sulfur containing ligands in two of the platinum(II) precursors was expected to result in a relatively lower activity. As a matter of fact, the most catalytically active systems were GM-69/230 (Pt content 2.9%) and GM-238/230 (Pt content 0.8%) originated from *trans*- $\text{Pt}(\text{O}_2\text{CNEt}_2)_2(\text{NHEt}_2)(\text{SEt}_2)$, and *trans*- $\text{Pt}(\text{O}_2\text{CNEt}_2)_2(\text{NHEt}_2)_2$, respectively. It is known³⁵ that the activity of structure-insensitive catalytic reactions is reduced in proportion to the amount of surface covered by sulfur; thus, it is not surprising that our values of catalytic activity are lower than those obtained, under the same experimental conditions, with a commercially available palladium heterogeneous catalyst. On the other hand, within the context of this work, the catalytic test has been used as a further evidence of the presence of platinum particles on the support and no effort towards optimization has been made. It has been suggested^{1c} that catalytic properties are affected by the particle size and that a diameter of 20 Å, corresponding to about 400 metal atoms, represents a threshold value above which a change of catalytic properties should be noticed. The preparation of sulfur-free silica-supported platinum requires the use of a sulfur-free platinum(II) precursor containing carbamate groups, such as *trans*- $\text{Pt}(\text{O}_2\text{CNEt}_2)_2(\text{NHEt}_2)_2$. On the other hand, sulfur contamination has been reported to be compatible with the platinum-catalysed oxidation of CO by dioxygen.³⁶

Conclusions

This paper has shown the possibility of implanting platinum(II) on a commercially available silica support starting from some platinum(II) precursors, through the electrophilic reaction by the silanol groups on the reactive *N,N*-diethylcarbamato ligand. The resulting silica is a functionalized one, statistically containing one residual carbamate group per platinum. This implantation method is an alternative to others reported in the literature^{27c} and is superior in some respects, especially for its high site selectivity. Also, provided a high OH/Pt molar ratio is used, the yield of the liquid–solid reaction is quantitative; moreover, the activity of the silanol groups is kept to a maximum, since solvents of low polarity can be used. Thus, by this method, platinum(II) can be implanted on silica at practically any required platinum content, up to a maximum of ca. 6%, as a function of the OH/Pt molar ratio. It has also been shown that the same mother platinum(II) solution can undergo progressive depletion by silica, and thus be used to prepare samples with different Pt contents. Formation of platinum nanoparticles has been achieved either thermally or with dihydrogen under mild conditions and the resulting

reduced system has been found to be active in the catalytic hydrogenation of cyclohexene.

This work was partly supported by the Consiglio Nazionale delle Ricerche (C.N.R., Roma), Progetto Strategico 'Tecnologie Chimiche Innovative'. We are indebted to Chimet SpA, Badia al Pino, Arezzo, Italy, for a sample of their commercially available oxide-supported hydrogenation catalyst and for a loan of platinum. One of us (G. M.) thanks ENI for a fellowship within the PhD programme at the Scuola Normale Superiore di Pisa (Perfezionamento in Scienze Molecolari Applicate).

References

- (a) L. Abis, D. Belli Dell' Amico, F. Calderazzo, R. Caminiti, F. Garbassi, S. Ianelli, G. Pelizzi, P. Robino and A. Tomei, *J. Mol. Catal.*, 1996, **108**, L113; (b) P. Rabette, A. M. Deane, A. J. Tench and M. Che, *Chem. Phys. Lett.*, 1979, **60**, 348; (c) M. Che and C. O. Bennett, *Adv. Catal.*, 1989, **36**, 55.
- (a) E. Agostinelli, D. Belli Dell' Amico, F. Calderazzo, D. Fiorani and G. Pelizzi, *Gazz. Chim. Ital.*, 1988, **118**, 729; (b) P. B. Arimondo, F. Calderazzo, U. Englert, C. Maichle-Mössmer, G. Pampaloni and J. Strähle, *J. Chem. Soc., Dalton Trans.*, 1996, 311; (c) D. Belli Dell' Amico, F. Calderazzo, F. Marchetti and G. Pampaloni, *Stoichiometric and Exhaustive Hydrolysis of N,N-Dialkylcarbamates*, in *Aqueous Organometallic Chemistry and Catalysis*, ed. I. T. Horváth and F. Joó, Kluwer Academic, Dordrecht-Boston-London, 1995 and references therein; (d) D. Belli Dell' Amico, F. Calderazzo and G. Pampaloni, *Chem. Rev.*, to be submitted.
- Handbook of Chemistry and Physics*, ed. D. R. Lide, 75th ed., CRC Press, Boca Raton-Ann Arbor-London-Tokyo, 1994-1995, p. 8-21.
- L. Abis, D. Belli Dell' Amico, C. Busetto, F. Calderazzo, R. Caminiti, F. Garbassi and A. Tomei, manuscript in preparation.
- J. Schwartz, *Acc. Chem. Res.*, 1985, **18**, 302; P. Dufour, C. C. Santini, C. Houtman and J. M. Basset, *J. Mol. Catal.*, 1991, **66**, L23; T. J. Marks, *Acc. Chem. Res.*, 1992, **25**, 57; F. Quignard, C. Lecuyer, C. Bougault, F. Lefebvre, A. Choplin, D. Olivier and J.-M. Basset, *Inorg. Chem.*, 1992, **31**, 928; P. Dufour, C. Houtman, C. C. Santini, C. Nédez, J. M. Basset, L. Y. Hsu and S. G. Shore, *J. Am. Chem. Soc.*, 1992, **114**, 4248; F. Quignard, C. Lecuyer, C. Bougault, F. Lefebvre, A. Choplin, D. Olivier and J. M. Basset, *Inorg. Chem.*, 1992, **31**, 928; P. Dufour, S. L. Scott, C. C. Santini, F. Lefebvre and J. M. Basset, *ibid.*, 1994, **33**, 2509; M. Taoufik, C. C. Santini, J.-P. Candy, A. de Mallmann and J. M. Basset, *J. Am. Chem. Soc.*, 1996, **118**, 4167; V. Vidal, A. Théolier, J. Thivolle-Cazat, J.-M. Basset and J. Croker, *ibid.*, 1996, **118**, 4595.
- B. Kauffman and D. O. Cowan, *Inorg. Synth.*, 1960, **6**, 211.
- Yu. N. Kukushkin and S. C. Dhara, *Indian J. Chem.*, 1970, **8**, 184; F. D. Rochon and P. C. Kong, *Can. J. Chem.*, 1986, **64**, 1894.
- (a) B. Sanna, Thesis, Degree in Chemistry, Università di Pisa, 1992-1993; (b) L. Marchetti, Thesis, Degree in Chemistry, Università di Pisa, 1994-1995.
- R. Alessio, D. Belli Dell' Amico, F. Calderazzo and U. Englert, *Gazz. Chim. Ital.*, 1993, **123**, 719.
- (a) J. B. Peri, *J. Phys. Chem.*, 1966, **70**, 2937 and references therein; (b) F. Boccuzzi, S. Coluccia, G. Ghiotti, C. Morterra and A. Zecchina, *ibid.*, 1978, **82**, 1298; (c) B. A. Morrow and A. J. McFarlan, *ibid.*, 1992, **96**, 1395; (d) A. Zecchina, S. Bordiga, G. Spoto, L. Marchese, G. Petrini, G. Leofanti and M. Padovan, *ibid.*, 1992, **96**, 4991; (e) *ibid.*, 1992, **96**, 4985 (f) A. Zecchina and C. O. Arian, *Catal. Rev. Sci. Eng.*, 1993, **35**, 261.
- (a) G. E. Maciel and D. W. Sindorf, *J. Am. Chem. Soc.*, 1980, **102**, 7606; (b) D. W. Sindorf and G. E. Maciel, *ibid.*, 1983, **105**, 1487; (c) *J. Phys. Chem.*, 1983, **87**, 5516; (d) *J. Am. Chem. Soc.*, 1983, **105**, 3767.
- F. Calderazzo and F. A. Cotton, *Inorg. Chem.*, 1962, **1**, 30.
- J. F. Moulder, W. F. Stickle, P. E. Sobol and K. D. Bomben, *Handbook of X-Ray Photoelectron Spectroscopy*, ed. J. Chastain, Perkin-Elmer Corporation, Eden Prairie, MN, 1994.
- (a) R. Caminiti, C. Sadun, V. Rossi, F. Cilloco and R. Felici, *25th Italian Congress of Physical Chemistry*, Cagliari, Italy, June 17-21, 1991; *Ital. Pat. Appl.* RM/93 A000410, June 23rd, 1993; (b) M. Carbone, R. Caminiti and C. Sadun, *J. Mater. Chem.*, 1996, **6**, 1709.
- R. W. James, *The Optical Principles of the Diffraction of X-Rays*, G. Bell & Sons Ltd, London, 1950.
- C. E. Briant, G. R. Hughes, P. C. Minshall and D. M. P. Mingos, *J. Organomet. Chem.*, 1980, **202**, C18.
- R. D. Shannon, *Acta Crystallogr., Sect. A*, 1976, **32**, 751.
- A. Anillo, D. Belli Dell' Amico, F. Calderazzo, M. Nardelli, G. Pelizzi and L. Rocchi, *J. Chem. Soc., Dalton Trans.*, 1991, 2845.
- O. Glatter and O. Kratky, *Small Angle X-Ray Scattering*, Academic Press, London, 1982.
- We thank Prof. G. Pelizzi, Università di Parma, for this X-ray experiment on a single crystal of *trans*-Pt(O₂CNET₂)₂(NHET₂)₂.
- See ref. 3, p. 8-45.
- (a) F. Basolo and R. G. Pearson, *Mechanisms of Inorganic Reactions*, J. Wiley, New York-London-Sydney, 2nd edn., 1967; (b) M. L. Tobe, *Inorganic Reaction Mechanisms*, Nelson, London, 1972.
- Y. Asakura, M. Yamada, and Y. Iwasawa, *Chem. Lett.*, 1985, 511.
- H. F. J. van't Blik, J. B. A. D. van Zon, T. Huizinga, J. C. Vis, D. C. Koningsberger and R. Prins, *J. Am. Chem. Soc.*, 1985, **107**, 3139.
- N. Binsted, J. Evans, G. N. Greaves and R. J. Price, *Organometallics*, 1989, **8**, 613.
- P. S. Kirilin, F. B. M. van Zon, D. C. Koningsberger and B. C. Gates, *J. Phys. Chem.*, 1990, **94**, 8439.
- (a) J. R. Chang, L. U. Gron, A. Honji, K. M. Sanchez and B. C. Gates, *J. Phys. Chem.*, 1991, **95**, 9944; (b) A. Masson, B. Bellamy, G. Colomer, M. M'bedi, P. Rabette and M. Che, *Proc. Int. 8th Congr. Catal.*, 1984, **4**, 333; quoted from ref. 1(c), p. 75; (c) S. D. Jackson, J. Willis, G. D. McLellan, G. Webb, M. B. T. Keegan, R. B. Moyes, S. Simpson, P. B. Wells and R. Whyman, *J. Catal.*, 1993, **139**, 191; (d) M. Muhler, Z. Paal and R. Schlögl, *Appl. Surf. Sci.*, 1991, **47**, 281; (e) D. M. Hercules and J. C. Klein, *Electron Spectroscopy for Chemical Analysis Applied to Heterogeneous Catalysis*, in *Applied Electron Spectroscopy for Chemical Analysis*, ed. H. Windawi and F. F.-L. Ho, J. Wiley, New York, NY, 1982, p. 147.
- R. R. Schrock and G. W. Parshall, *Chem. Rev.*, 1976, **76**, 243.
- (a) J. M. Mayer, C. J. Curtis and J. E. Bercaw, *J. Am. Chem. Soc.*, 1983, **105**, 2651; (b) G. Parkin, E. Bunel, B. J. Burger, M. S. Trimmer, A. van Asselt and J. E. Bercaw, *J. Mol. Catal.*, 1987, **41**, 21.
- (a) H. E. Bryndza, J. C. Calabrese, M. Marsi, D. C. Roe, W. Tam and J. E. Bercaw, *J. Am. Chem. Soc.*, 1986, **108**, 4805; (b) A. Sacco and P. Mastroianni, *J. Chem. Soc., Dalton Trans.*, 1994, 2761; (c) O. Blum and D. Milstein, *J. Am. Chem. Soc.*, 1995, **117**, 4582.
- (a) V. B. Kazansky, V. Yu. Borovkov, N. Sokolova, N. I. Jaeger and G. Schulz-Ekloff, *Catal. Lett.*, 1994, **23**, 263; (b) C. Besoukhanova, J. Guidot and D. Barthomeuf, *J. Chem. Soc., Faraday Trans.*, 1981, **77**, 1595; (c) R. P. Eischens and W. A. Pliskin, *Adv. Catal.*, 1958, **10**, 1; (d) T. M. Tri, J.-P. Candy, P. Gallezot, J. Massardier, M. Primet, J. C. Védrine and B. Imelik, *J. Catal.*, 1983, **79**, 396; (e) C. De La Cruz and N. Sheppard, *Spectrochim. Acta, Part A*, 1994, **50**, 271; (f) M. Vaarkamp, B. L. Mojet, M. J. Kappers, J. T. Miller and D. C. Koningsberger, *J. Phys. Chem.*, 1995, **99**, 16067; (g) J. C. Calabrese, L. F. Dahl, A. Cavalieri, P. Chini, G. Longoni and S. Martinengo, *J. Am. Chem. Soc.*, 1974, **96**, 2614; (h) G. Longoni and P. Chini, *ibid.*, 1976, **98**, 7225; (i) D. M. Washecheck, E. J. Wucherer, L. F. Dahl, A. Ceriotti, G. Longoni, M. Manassero, M. Sansoni and P. Chini, *ibid.*, 1979, **101**, 6110; (j) D. M. P. Mingos and R. W. M. Wardle, *Transition Met. Chem.*, 1985, **10**, 441.
- JCPDS, Joint Committee on Powder Diffraction Standards, 1601 Park Lane, Swarthmore, PA, Card No. 4-0802.
- (a) T. E. Whyte, Jr., *Catal. Rev.*, 1973, **8**, 117; (b) T. Gacoin, F. Chaput, J. P. Boilot and G. Jaskierowicz, *Chem. Mater.*, 1993, **5**, 1150.
- (a) J. P. Bucher, J. Buttet, J. J. van der Klink and M. Graetzel, *Surf. Sci.*, 1989, **214**, 347; (b) Y. Takasu, M. Teramoto and Y. Matsuda, *J. Chem. Soc., Chem. Commun.*, 1983, 1329.
- (a) M. Boudart, A. Aldag, J. E. Benson, N. A. Dougharty and C. G. Harkins, *J. Catal.*, 1966, **6**, 92; (b) G. Leclercq and M. Boudart, *ibid.*, 1981, **71**, 127.
- (a) R. F. Baddour, M. Modell and R. L. Goldsmith, *J. Phys. Chem.*, 1970, **74**, 1787; (b) T. Engel and G. Ertl, *Adv. Catal.*, 1979, **28**, 1.

Paper 7/053331; Received July 23rd, 1997